Stability of a half-quantum vortex in rotating superfluid ^{3}He-*A* between parallel plates

T. Kawakami, Y. Tsutsumi, and K. Machida
Department of Physics, Okayama University, Okayama 700-8530, Japan
(Received 12 February 2009; published 30 March 2009)

We have found the precise stability region of the half quantum vortex (HQV) for superfluid ^{3}He-*A* phase confined in parallel plates with a narrow gap under rotation. Standard Ginzburg-Landau free energy, which is well established, is solved to locate the stability region spanned by temperature T and rotation speed (Ω). This Ω-T stability region is wide enough to check it experimentally in available experimental setup. The detailed order-parameter structure of HQV characterized by A_1 core is given to facilitate the physical reasons of its stability over other vortices or textures.

DOI: 10.1103/PhysRevB.79.092506 PACS number(s): 67.30.he, 67.30.ht, 71.10.Pm

Half quantum vortex (HQV) and associated Majorana zero energy mode have been widely discussed in various research fields in condensed-matter physics, ranging from superconductors, superfluids, graphene, and fractional Quantum Hall systems.[1] In particular, theoretical and experimental investigations are devoted to finding HQV in superconductors and neutral Fermion superfluids in cold atoms. Recently strong interest on HQV is partly motivated by the fact that the bound state created in the core of HQV is characterized by the Majorana state with the zero energy exactly at the Fermi level. The Majorana particle[2] is thought to be a candidate for quantum computation because it obeys non-Abelian statistics[3] and its existence is protected topologically to avoid decoherence. These situations are ideal for quantum computation[4] if it really exists.

So far there has been no firm experimental evidence for HQV in any superconductors. It is necessary for HQV to exist that superconductivity is described by a chiral p-wave pairing. The $\vec{d}$ vector, which denotes the perpendicular direction of the Cooper pair spin, is able to be free to rotate. It has often been argued that Sr_2RuO_4 may be a prime candidate,[5–7] but strong doubt has been cast on this possibility of Sr_2RuO_4 of its triplet pairing.[8–10] Note that the first discovered triplet superconductor UPt_3 is an f-wave pairing, not chiral p-wave.[11]

Superfluid ^{3}He-*A* phase is characterized by a chiral p-wave pairing. There is no doubt on this identification.[12] In fact, Volovik and Mineev[13] are the first to point out the possibility to the realization of HQV in 1976. Since then, there have been several general arguments on the stability of a HQV in connection with ^{3}He-*A* phase.[14–16] However, there are no serious calculations which consider realistic situation in superfluid ^{3}He-*A* phase on how to stabilize it and on what boundary conditions are needed for it.

Recently, Yamashita *et al.*[17] have performed an experiment intended to observe HQV in superfluid ^{3}He-*A* in parallel-plate geometry. The superfluid is confined in a cylindrical region with the radius $R=1.5$ mm and the height 12.5 μm sandwiched by parallel plates. A magnetic field $H=26.7$ mT($\|z$) is applied perpendicular to the parallel plates under pressure $P=3.05$ MPa. Since the gap 12.5 μm between plates is narrow compared to the dipole coherence length $\xi_d \sim 10$ μm, the $\vec{l}$ vector, which signifies the direction of orbital angular momentum of Cooper pairs, is always perpendicular to the plates. Also the $\vec{d}$ vector is confined within the plane because the dipole magnetic field $H_d \sim 2.0$ mT,[12] where H tends to align the $\vec{d}$ vector perpendicular to the field direction. They investigate to seek out various parameter spaces, such as temperature T, or the rotation speed Ω up to $\Omega=6.28$ rad/s by using the rotating cryostat in ISSP, Univ. Tokyo, capable for the maximum rotation speed ~ 12 rad/s, but there is no evidence for HQV.[17] Here we are going to give an answer why it is so and to examine the stability region of a HQV which competes with the ordinary singular vortex with the integer winding number and propose a concrete experimental setup which is feasible to perform in the light of the present experimental situation.[17]

We start out by examining the possible order parameter (OP) forms allowed under the above experimental conditions. The most general OP of triplet pairing is written by

$$\hat{\Delta}(\mathbf{r},\hat{\mathbf{p}}) = \begin{pmatrix} \Delta_{\uparrow\uparrow}(\mathbf{r},\hat{\mathbf{p}}) & \Delta_{\uparrow\downarrow}(\mathbf{r},\hat{\mathbf{p}}) \\ \Delta_{\downarrow\uparrow}(\mathbf{r},\hat{\mathbf{p}}) & \Delta_{\downarrow\downarrow}(\mathbf{r},\hat{\mathbf{p}}) \end{pmatrix} = \frac{1}{\sqrt{2}} \begin{pmatrix} -d_x(\mathbf{r},\hat{\mathbf{p}}) + id_y(\mathbf{r},\hat{\mathbf{p}}) & d_z(\mathbf{r},\hat{\mathbf{p}}) \\ d_z(\mathbf{r},\hat{\mathbf{p}}) & d_x(\mathbf{r},\hat{\mathbf{p}}) + id_y(\mathbf{r},\hat{\mathbf{p}}) \end{pmatrix}, \tag{1}$$

where $\hat{\mathbf{p}}$ is the unit vector of the momentum on the Fermi surface. We can put $\Delta_{\uparrow\downarrow}(\mathbf{r},\hat{\mathbf{p}})=\Delta_{\downarrow\uparrow}(\mathbf{r},\hat{\mathbf{p}})=0$ under applied fields greater than the dipole magnetic field. Thus OP is reduced to

$$\hat{\Delta}(\mathbf{r},\hat{\mathbf{p}}) = \begin{pmatrix} A_{\uparrow+}(r,\theta)\hat{p}_+ + A_{\uparrow-}(r,\theta)\hat{p}_- & 0 \\ 0 & A_{\downarrow+}(r,\theta)\hat{p}_+ + A_{\downarrow-}(r,\theta)\hat{p}_- \end{pmatrix}, \tag{2}$$

where $\hat{p}_\pm = \mp \frac{1}{\sqrt{2}}(\hat{p}_x \pm i\hat{p}_y)$ and $d_\mu(\mathbf{r},\hat{\mathbf{p}})=A_{\mu i}(\mathbf{r})\hat{p}_i$ ($\mu=\uparrow,\downarrow$, $i=\pm$). We have suppressed the $\hat{p}_z$ component because the boundary condition of the parallel plate inhibits nonvanishing $\hat{p}_z$ component. Since in the superfluid ^{3}He-*A* phase, characterized by the separable form of the spin part and the orbital part $\hat{\mathbf{p}}$,[12] under weak magnetic fields the up- and down-spin spaces are degenerate, it can be expressed also by restoring the **d** vector for a moment as

$$\hat{\Delta}(\mathbf{r},\hat{\mathbf{p}}) = \begin{pmatrix} A_+(\mathbf{r})\hat{d}_\uparrow\hat{p}_+ & 0 \\ 0 & A_+(\mathbf{r})\hat{d}_\downarrow\hat{p}_+ \end{pmatrix}, \tag{3}$$

where $A_\pm(\mathbf{r}) = \mp\frac{1}{\sqrt{2}}[A_x(\mathbf{r}) \mp iA_y(\mathbf{r})]$, $\hat{d}_\uparrow = -\frac{1}{\sqrt{2}}(\hat{d}_x - i\hat{d}_y)$, $\hat{d}_\downarrow = \frac{1}{\sqrt{2}}(\hat{d}_x + i\hat{d}_y)$, and $A_+(\mathbf{r}) = A_+(r)e^{i\Phi}$, where Φ is the phase of the orbital part.

The HQV proposed by Salomaa and Volovik[14] and others[3,5,7] can be described by $\Phi = \theta/2$ and $\hat{\mathbf{d}} = \hat{\mathbf{x}}\cos(\theta/2) - \hat{\mathbf{y}}\sin(\theta/2)$ of Eq. (3) in the polar coordinates (r,θ). This means physically that the $\uparrow\uparrow$ pairs phase wind by 2π while the $\downarrow\downarrow$ pairs do not. When winding the vortex core by 2π the HQV maps to itself by simultaneous change in the sign of the $\hat{\mathbf{d}}$ and the π phase shift, $(\Phi,\hat{\mathbf{d}}) \Rightarrow (\Phi+\pi,-\hat{\mathbf{d}})$. Here the $\hat{\mathbf{d}}$ vector is assumed to be real, we call it R-HQV. It will turn out shortly that this somewhat restrictive R-HQV form is not a full solution of our Ginzburg-Landau (GL) free-energy functional under rotation.

Thus we have to seek more general HQV solution to be competitive with the vortex free state stable at rest [A phase texture (AT)] and the singular vortex (SV) with integer winding. We examine the more general OP given by Eq. (2) to find the stable HQV by noticing that the orbital part is doubly degenerate $p_\pm$ in addition to doubly degenerate spin space in the A phase. Here each component $A_{\uparrow\pm}(\mathbf{r}) = A_{\uparrow\pm}(r)e^{i\theta w_{\uparrow\pm}}$ and $A_{\downarrow\pm}(\mathbf{r}) = A_{\downarrow\pm}(r)e^{i\theta w_{\downarrow\pm}}$ can have its own winding number $w_{\uparrow\pm}$ and $w_{\downarrow\pm}$. Under axis-symmetry $w_{\uparrow+} = w_{\uparrow-} - 2$ and $w_{\downarrow+} = w_{\downarrow-} - 2$ must be satisfied.[18] The winding number combination $(w_{\uparrow+}, w_{\downarrow+}, w_{\uparrow-}, w_{\downarrow-}) = (1,0,3,2)$ is straightforwardly generalized from the above R-HQV form (3), which we are trying to stabilize. The (0,0,2,2) phase is the A phase texture and (1,1,3,3) is the ordinary singular vortex. The AT is always stable at rest, and HQV and SV compete each other under rotation. Other several phases with different winding number combinations, such as $(0,-1,2,1)$, $(-1,-2,1,0)$, or $(-1,-1,1,1)$ are all irrelevant; namely, they are never stabilized. Note that the $(0,-1,2,1)$ phase is stable next to the lowest AT (0,0,2,2) at rest. Under counterclockwise rotation the chiral p_+ is favored over p_-. Thus the p_+ (p_-) component constitutes the major (minor) one.

The Ginzburg-Landau free-energy functional invariant under gauge transformation, spin, and orbital space rotations is well established[12,15,19–21] and given by a standard form

$$f_{\text{total}} = f_{\text{grad}} + f_{\text{bulk}} + f_{\text{dipole}}, \tag{4}$$

$$f_{\text{grad}} = K[(\partial_i^* A_{\mu j}^*)(\partial_i A_{\mu j}) + (\partial_i^* A_{\mu j}^*)(\partial_j A_{\mu i}) + (\partial_i^* A_{\mu i}^*)(\partial_j A_{\mu j})], \tag{5}$$

$$f_{\text{bulk}} = -\alpha_\mu A_{\mu i}^* A_{\mu i} + \beta_1 A_{\mu i}^* A_{\mu i}^* A_{\nu j} A_{\nu j} + \beta_2 A_{\mu i}^* A_{\nu j}^* A_{\mu i} A_{\nu j} + \beta_3 A_{\mu i}^* A_{\nu i}^* A_{\mu j} A_{\nu j} + \beta_4 A_{\mu i}^* A_{\nu j}^* A_{\mu j} A_{\nu i} + \beta_5 A_{\mu i}^* A_{\mu j}^* A_{\nu i} A_{\nu j}, \tag{6}$$

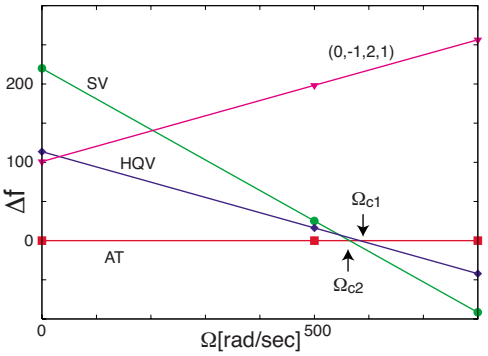

FIG. 1. (Color online) Free-energy comparison for AT, HQV, SV and $(0,-1,2,1)$ states as a function of Ω for $R=10$ μm and $t = T/T_c = 0.97$. Δf is the relative free energy to AT.

$$f_{\text{dipole}} = g_d\left(A_{\mu\mu}^* A_{\nu\nu} + A_{\mu\nu}^* A_{\nu\mu} - \frac{2}{3}A_{\mu\nu}^* A_{\mu\nu}\right), \tag{7}$$

where $\partial_i = \nabla_i - i\frac{2m_3}{\hbar}(\vec{\Omega}\times\vec{r})_i$ $(\vec{\Omega}\|z)$, $\mu,i = x,y$. The quadratic term $-\alpha_\mu A_{\mu i}^* A_{\mu i} = -\alpha_\sigma A_{\sigma i}^* A_{\sigma i}$ $(\sigma = \uparrow,\downarrow)$ with $\alpha_\sigma = \alpha_0(1 - T/T_c - \sigma\Delta T/T_c)$ $(\alpha_0 = \frac{N(0)}{3})$. $K = 7\zeta(3)N(0)(\hbar v_F)^2/240(\pi k_B T_c)^2$. g_d is the coupling constant of the dipole interaction, which is $g_d \ll \alpha_0$.[12] As mentioned above, we assume a two-dimensional system for the OP spatial variation. The magnetic field acts not only to pin the $\vec{d}$ vector within the plane, but also to shift the transition temperature T_c by $\Delta t = \Delta T/T_c = (T_{c\downarrow} - T_{c\uparrow})/2T_c$. The fourth-order GL coefficients are given by $\beta_1 = -(1+0.1\delta)\beta_0$, $\beta_2 = (2+0.2\delta)\beta_0$, $\beta_3 = (2-0.05\delta)\beta_0$, $\beta_4 = -(2-0.055\delta)\beta_0$, and $\beta_5 = -(2+0.7\delta)\beta_0$ where $\beta_0 = 7\zeta(3)N(0)/120(\pi k_B T_c)^2$.[15] The strong-coupling correction $\delta > 0$ due to spin fluctuations serves stabilizing the A phase over the B phase in the (P,T) phase diagram.[22] In the following we use the GL parameters[23] tabulated[19–21] appropriate for the experiment at $P = 3.05$ MPa.

We find the free-energy minima under the rigid boundary condition $A_{\mu i} = 0$ for $r \geq R$ (R is the radius of the system). A fundamental difficulty associated with the numerical computations lies in the fact that the coherent length $\xi = 10$ nm is extremely small compared with the system size R where we have to take care of these two length scales in the equal footing in order to accurately evaluate the relative stability among three textures; AT, HQV, and SV. This is a reason why this kind of serious energy comparison has not been done before. We carefully calibrate the accuracy of our numerical computation to allow the detailed comparison.

We first consider the weak-field case where the transition temperature splitting $\Delta t \simeq 0$. As shown in Fig. 1 we compare three phases with additional other phase mentioned above. It is seen that at rest and lower rotation region AT is stable and eventually upon increasing Ω, SV takes over at Ω_{c2}. Although the HQV is more stable than SV at rest situated almost at the half way between AT and SV because the phase winding occurs only for the $\uparrow\uparrow$ pairs. Under rotation the energy gain due to the angular momentum is less than that in SV because of the above reason. Thus HQV is never stabilized under weak-field region. We also plot the $(0,-1,2,1)$

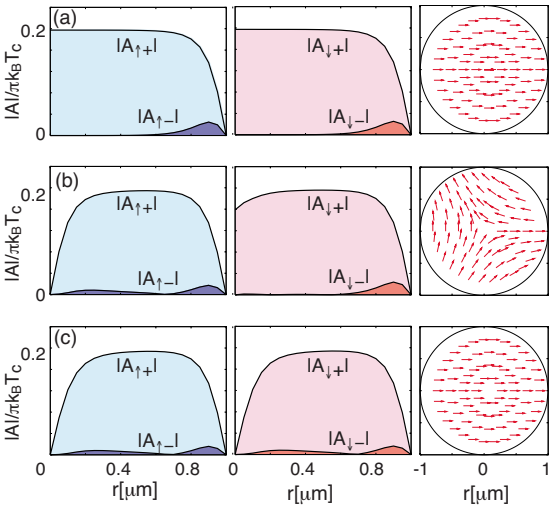

FIG. 2. (Color online) Order parameter amplitude $|A|$ normalized by $\pi k_B T_c$ and $\hat{\mathbf{d}}$ vector profiles for (a) AT, (b) HQV, and (c) SV for $R=1.0$ μm and $t=0.97$. Left and center columns show the cross section of OP along the radial direction r. Right column shows $\hat{\mathbf{d}}$ vector patterns. In (b) it winds by π around the center $r=0$.

state which is second lowest at rest and becomes irrelevant under rotation.

Note that the previous form (3) of R-HQV does not improve this situation, rather becomes worse in its stability. The R-HQV (3) indicates that the vortex core singularity occurs for both $\uparrow\uparrow$ and $\downarrow\downarrow$ pairs even though the latter does not have phase winding, leading to the additional loss of the condensation energy. The strong-coupling effect acts to destabilize both R-HQV and SV relative to AT, thus R-HQV is never stabilized (see below).

In Fig. 2 we illustrate the results of the OP profiles for (a) AT, (b) HQV, and (c) SV and their $\vec{d}$ vector textures. The OPs in AT are uniform in the central region around $r=0$, decreasing toward zero at the boundary $r=R$ whose characteristic length is ξ. Thus AT is basically the A phase in the bulk. Near the boundary the induced components $A_{\uparrow-}$ and $A_{\downarrow-}$ appear peripherally.

In HQV [Fig. 2(b)] one of the two majority components $A_{\uparrow+}$ with $w_{\uparrow+}=1$ exhibits a phase singularity at $r=0$, the other component $A_{\downarrow+}$ with $w_{\downarrow+}=0$ being depressed slightly there. $A_{\uparrow-}$ with $w_{\uparrow-}=3$ and $A_{\downarrow-}$ with $w_{\downarrow-}=2$ are also induced at $r=0$ and $r=R$. Therefore this HQV profile shows that only the $\downarrow\downarrow$ pairs appears at around $r=0$, implying the A_1 core state. This tends to stabilize this HQV further compared with R-HQV given by Eq. (3) because (A) the condensation energy loss is less, (B) the fourth order GL energy concerning the interaction term between $\uparrow\uparrow$ and $\downarrow\downarrow$ pairs can be expressed as $-4\delta\beta_0|\hat{d}_\uparrow|^2|\hat{d}_\downarrow|^2$. This particular term due to the strong-coupling acts to earn the extra gain for this HQV. However, AT is simultaneously stabilized by this term, thus HQV never wins in weak fields. Note in passing that the $\uparrow\uparrow$ and $\downarrow\downarrow$ pairs are completely independent when $\delta=0$ because the weak-coupling GL form is derived under the assumption that the spin space is rotationally invariant. It is seen from Fig. 2 that the $\vec{d}$ vector rotates by π when going around the origin in (b) HQV while in the [(a) and (c)] others it is uniform.

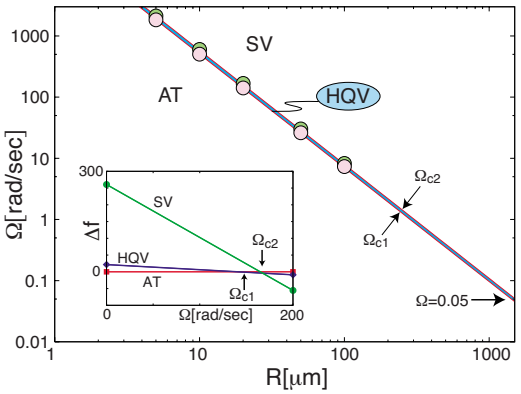

FIG. 3. (Color online) Stability region of HQV sandwiched between Ω_{c1} and Ω_{c2} as a function of R ($t=0.97$ and $\Delta t=0.05$). $\Omega_{c1}=0.05$ rad/s is the extrapolated value for $R=1.5$ mm. Inset shows the free-energy comparison for $R=20$ μm, displaying the successive transitions from AT to HQV at Ω_{c1} and from HQV to SV at Ω_{c2}.

Finally SV in Fig. 2(c) exhibits the phase singularities for both major components $A_{\uparrow+}$ with $w_{\uparrow+}=1$ and $A_{\downarrow+}$ with $w_{\downarrow+}=1$ and the induced components $A_{\uparrow-}$ with $w_{\uparrow-}=3$ and $A_{\downarrow-}$ with $w_{\downarrow-}=3$ appear at the places where the OP spatially varies. Thus this SV is quite advantageous under rotation because they can absorb efficiently the rotational kinetic energy.

Having found that HQV is not stable in weak-field region ($H\sim H_d=10$ mT) both at rest and under rotation, we resort to higher field region; an order of a few kG where $\Delta t\neq 0$ or $T_{c\uparrow}\neq T_{c\downarrow}$. This extension indeed stabilizes the HQV as shown in the inset of Fig. 3 where we compare the three states as a function of Ω. It is seen that as increasing Ω, AT changes into HQV at Ω_{c1} and then HQV to SV at Ω_{c2}. The relative stability region $\Omega_{c1}/\Omega_{c2}\sim 0.85$ which is wide enough to check experimentally.

The reason for the HQV stabilization is physically explained as follows. By introducing Δt which increases (decreases) the OP amplitude of $\downarrow\downarrow$ pair ($\uparrow\uparrow$ pair), the kinetic-energy loss due to the phase winding of $A_{\uparrow+}$ with $w_{\uparrow+}=1$, which remains unscreened and spreads out whole system, becomes less compared to AT at rest, meaning that the HQV energy approaches toward the AT energy in Fig. 1 at $\Omega=0$ as seen from inset of Fig. 3. Under rotation the HQV energy decreases by absorbing the rotation kinetic energy and eventually becomes lower at Ω_{c1}, which is smaller than Ω_{c2}, stabilizing HQV over SV.

The main panel in Fig. 3 shows Ω_{c1} and Ω_{c2} as a function of the system size R. It is seen that the relative stability region $\Omega_{c1}/\Omega_{c2}\sim 0.85$ stays at a constant against R, keeping 15% region above the critical rotation speed Ω_{c1} at which single HQV is created in the system. The extrapolated Ω_{c1} to $R=1.5$ mm, by which Yamashita *et al.*[17] have performed experiments, amounts to $\Omega_{c1}\sim 0.05$ rad/s. The rotation speed stability of the rotation cryostat at ISSP, Univ. Tokyo is accurate enough to perform it. We also notice that by changing the radius R of the system one can control the Ω_{c1} value at

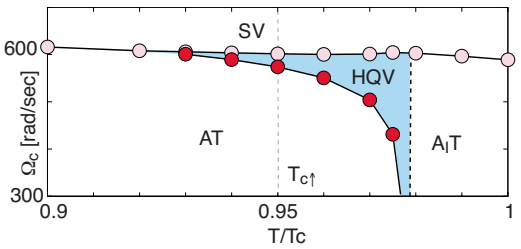

FIG. 4. (Color online) Stability region of HQV in Ω versus T/T_c ($R=10$ μm and $\Delta t=0.05$). A_1T denotes the A_1 phase texture where only $\downarrow\downarrow$ pairs exist.

will. For example, in $R=300$ μm, $\Omega_{c1}\sim 1$ rad/s which is convenient speed to run their rotating cryostat.

In Fig. 4 we depict the temperature dependence of the HQV stability region. We see that the stability region for HQV is widen divergently when approaching the lower critical temperature $T_{c\uparrow}$ from below where the disparity of the OP amplitudes between $\uparrow\uparrow$ pair and $\downarrow\downarrow$ pair increases. Note that the actual lower transition temperature $T_{c\uparrow}$ is shifted slightly upward because the spatially varying $\uparrow\uparrow$ pair OP $A_{\downarrow+}(r)$ induces $A_{\uparrow+}(r)$. In other words, the A_1 phase for $T_{c\downarrow}>T>T_{c\uparrow}$ becomes narrower. Thus one needs not only careful temperature control, an order of 0.01 K which is feasible enough, but also theoretical backup to estimate this shift in order to precisely locate the HQV stability region under actual experimental setup.

Since the HQV has the odd winding number for the $\uparrow\uparrow$ pairs, the Majorana quasiparticle with zero energy exactly at the Fermi level, which is localized in the vortex core, is ensured by both the index theorem based on topological argument,[24] or directly solving the Bogoliubov-de Gennes equation.[25] These arguments are based on the assumption that the $\uparrow\uparrow$ pair and $\downarrow\downarrow$ pair are completely decoupled. Here the situation is more subtle. The $\uparrow\uparrow$ pair and $\downarrow\downarrow$ pair are interacting through the fourth-order GL terms, which is mentioned above. These terms comes from the strong-coupling effect due to ferromagnetic spin fluctuations,[22] which ultimately help stabilizing the present HQV. Therefore, it is not obvious completely that the present HQV can accommodate the Majorana fermion with the exactly zero energy. This issue belongs to a future problem.

We also remark on the experimental point that the identification of the HQV is not an easy task. The HQV and SV are indistinguishable by the usual NMR method which utilizes the satellite position in the spectrum[17] because $\vec{d}\perp\vec{l}$ is always kept for both vortices, giving rise to the identical NMR spectra. We suggest small tilting of the field direction from $H\|z$ may yield the different NMR signatures. This point deserves further elaboration.

Finally it should be pointed out that our previous theory for the parallel geometry of the superfluid ^{3}He (Ref. 25) differs in the field orientation $H\perp z$ there. The singular vortex with odd integer winding number was found in this spinless chiral superfluid. This also gives rise to the Majorana zero energy mode. Thus the field orientations yield different vortices, but those accommodate the Majorana particle localized at each vortex core.

In conclusion, we have found the stability region of half quantum vortex in T-Ω plane of superfluid ^{3}He-A phase confined in parallel plates and given physical reasons why it is more stable than A phase texture or ordinary singular vortex. We propose a concrete experimental setup, which is feasible by using the rotating cryostat such as in ISSP, Univ. Tokyo.

We thank T. Ohmi, O. Ishikawa, M. Yamashita, R. Ishiguro, K. Izumina, M. Kubota, T. Mizushima, M. Ichioka, and G. E. Volovik for useful discussions.

[1] L. Fu and C. L. Kane, Phys. Rev. Lett. **100**, 096407 (2008); P. Ghaemi and F. Wilczek, arXiv:0709.2626 (unpublished); J. Nilsson *et al.*, Phys. Rev. Lett. **101**, 120403 (2008); D. L. Bergman and K. Le Hur, arXiv:0806.0379 (unpublished).
[2] *Ettore Majorana*, edited by G. F. Bassani and the Council of the Italian Physical Society (Springer, Heidelberg, 2006).
[3] D. A. Ivanov, Phys. Rev. Lett. **86**, 268 (2001).
[4] S. C. Nayak *et al.*, Rev. Mod. Phys. **80**, 1083 (2008).
[5] H. Y. Kee, Y. B. Kim, and K. Maki, Phys. Rev. B **62**, R9275 (2000); Europhys. Lett. **80**, 46003 (2007).
[6] S. Das Sarma, C. Nayak, and S. Tewari, Phys. Rev. B **73**, 220502(R) (2006).
[7] S. B. Chung, H. Bluhm, and E. A. Kim, Phys. Rev. Lett. **99**, 197002 (2007).
[8] K. Machida and M. Ichioka, Phys. Rev. B **77**, 184515 (2008).
[9] A. G. Lebed and N. Hayashi, Physica C **341-348**, 1677 (2000).
[10] I. Žutić and I. Mazin, Phys. Rev. Lett. **95**, 217004 (2005).
[11] K. Machida *et al.*, J. Phys. Soc. Jpn. **58**, 4116 (1989); J. Phys. Soc. Jpn. **68**, 3364 (1999); J. A. Sauls, Adv. Phys. **43**, 113 (1994).
[12] A. J. Leggett, Rev. Mod. Phys. **47**, 331 (1975); D. Vollhardt and P. Wölfle, *The Superfluid Phase of Helium 3* (Taylor and Francis, London, 1990).
[13] G. E. Volovik and V. P. Mineev, JETP Lett. **24**, 561 (1976).
[14] M. C. Cross and W. F. Brinkman, J. Low Temp. Phys. **27**, 683 (1977); M. M. Salomaa and G. E. Volovik, Phys. Rev. Lett. **55**, 1184 (1985).
[15] M. M. Salomaa and G. E. Volovik, Rev. Mod. Phys. **59**, 533 (1987).
[16] G. E. Volovik, *Exotic Properties of Superfluid ^{3}He* (World Scientific, Singapore, 1992), p. 130.
[17] M. Yamashita *et al.*, Phys. Rev. Lett. **101**, 025302 (2008).
[18] T. Isoshima, K. Machida, and T. Ohmi, Phys. Rev. A **60**, 4857 (1999).
[19] J. A. Sauls and J. W. Serene, Phys. Rev. B **24**, 183 (1981).
[20] D. S. Greywall, Phys. Rev. B **33**, 7520 (1986).
[21] T. Kita, Phys. Rev. B **66**, 224515 (2002).
[22] P. W. Anderson and W. F. Brinkmann, Phys. Rev. Lett. **30**, 1108 (1973).
[23] The following GL parameters are used: $\alpha_0=3.81\times 10^{50}[J^{-1}m^{-3}]$, and $\beta_1=-3.75$, $\beta_2=6.65$, $\beta_3=6.56$, $\beta_4=5.99$, $\beta_5=-8.53$ in units of $10^{99}[J^{-3}m^{-3}]$.
[24] S. Tewari, S. Das Sarma, and D. H. Lee, Phys. Rev. Lett. **99**, 037001 (2007).
[25] Y. Tsutsumi *et al.*, Phys. Rev. Lett. **101**, 135302 (2008).